

# Genome-Wide Identification, Classification, and Expression Analysis of Autophagy-Associated Gene Homologues in Rice (*Oryza sativa* L.)

KUAIWEI Xia<sup>1,2</sup>, TAO Liu<sup>1,3</sup>, JIE Ouyang<sup>4</sup>, REN Wang<sup>1,3</sup>, TIAN Fan<sup>1,3</sup>, and MINGYONG Zhang<sup>1,\*</sup>

*Key Laboratory of Plant Resources Conservation and Sustainable Utilization, South China Botanical Garden, Chinese Academy of Sciences, Guangzhou 510650, PR China<sup>1</sup>; Key Laboratory of South China Agricultural Plant Genetics and Breeding, South China Botanical Garden, Chinese Academy of Sciences, Guangzhou 510650, PR China<sup>2</sup>; Graduate University of Chinese Academy of Sciences, Beijing 100049, PR China<sup>3</sup> and Chongqing Academy of Agricultural Sciences, Chongqing 401329, PR China<sup>4</sup>*

\*To whom correspondence should be addressed. Tel/Fax. +86 20-3725-2891. E-mail: zhangmy@scbg.ac.cn

Edited by Mikio Nishimura

(Received 30 March 2011; accepted 20 June 2011)

## Abstract

**Autophagy is an intracellular degradation process for recycling macromolecules and organelles. It plays important roles in plant development and in response to nutritional demand, stress, and senescence. Organisms from yeast to plants contain many autophagy-associated genes (ATG). In this study, we found that a total of 33 ATG homologues exist in the rice [*Oryza sativa* L. (*Os*)] genome, which were classified into 13 ATG subfamilies. Six of them are alternatively spliced genes. Evolutional analysis showed that expansion of 10 *OsATG* homologues occurred via segmental duplication events and that the occurrence of these *OsATG* homologues within each subfamily was asynchronous. The *Ka/Ks* ratios suggested purifying selection for four duplicated *OsATG* homologues and positive selection for two. Calculating the dates of the duplication events indicated that all duplication events might have occurred after the origin of the grasses, from 21.43 to 66.77 million years ago. Semi-quantitative RT-PCR analysis and mining the digital expression database of rice showed that all 33 *OsATG* homologues could be detected in at least one cell type of the various tissues under normal or stress growth conditions, but their expression was tightly regulated. The 10 duplicated genes showed expression divergence. The expression of most *OsATG* homologues was regulated by at least one treatment, including hormones, abiotic and biotic stresses, and nutrient limitation. The identification of *OsATG* homologues showing constitutive expression or responses to environmental stimuli provides new insights for in-depth characterization of selected genes of importance in rice.**

**Key words:** autophagy; rice; hormone; stress; gene family

## 1. Introduction

Autophagy is a highly evolutionarily conserved cellular degradation process common to organisms from yeast to plants and animals.<sup>1,2</sup> The autophagy process can be broken down into a series of steps, including induction, cargo recognition and packaging, vesicle nucleation, vesicle expansion and completion, autophagy-associated protein cycling, vesicle fusion

with the vacuole/lysosome, vesicle breakdown, and recycling of the macromolecules.<sup>2,3</sup> In the process, the macromolecules or organelles are sequestered into a double-membrane vesicle, called an autophagosome, and finally delivered into the vacuole/lysosome for breakdown.<sup>1,2</sup>

The genes involved in this pathway are called autophagy-associated genes (*ATG*). In yeast, at least 32 *ATGs* have been identified and shown to participate in the

autophagy process.<sup>1,4</sup> The knowledge concerning the machinery and molecular mechanism of autophagy mainly comes from yeast.<sup>1,2</sup> Autophagy is maintained at a basal level under normal growth conditions but can be induced in response to nutritional demand, biotic or abiotic stresses, and senescence, thereby relieving the cell from various stress conditions. Autophagy also plays a critical role during cellular development and differentiation.

Many orthologues of ATGs have been identified in higher eukaryotes. In *Arabidopsis thaliana*, 25 homologues to 12 yeast ATGs essential for autophagy have been discovered.<sup>5</sup> They have essentially similar biochemical roles as those in yeast.<sup>2</sup> In plants, autophagy is important in the formation and degradation of protein storage vacuoles during seed development and germination, *de novo* vacuolar biogenesis, nutrient recycling during starvation, senescence, apoptotic processes such as xylem and sclerid cell morphogenesis, and the pathogen-induced hypersensitive response.<sup>6</sup> Some of these roles have been demonstrated by the phenotypic analyses of ATG-knockdown transgenic plants. RNAi-*AtATG18a* transgenic plants are hypersensitive to oxidative stress, suggesting a physiological role for this gene in response to this stress.<sup>7</sup> When *Arabidopsis*-null mutants of *AtATG5*, *AtATG7*, *AtATG9*, and *AtATG4* are grown under either carbon- or nitrogen-deficient conditions, the mutants exhibit the abnormal phenotypes of chlorosis, bolting, and senescence.<sup>6</sup> *AtATG6* is essential for pollen germination, and disruption of *AtATG6* by T-DNA insertion causes male sterility, as *AtATG6*-deficient pollen develops normally but does not germinate.<sup>8</sup>

In the *Arabidopsis*, rice and corn (*Zea mays*) genomes, some ATG homologues have been found, indicating that comparable autophagy systems exist in plants.<sup>7,9</sup> However, there are some differences between plants and yeast in the number of paralogues of ATGs. The *Arabidopsis* genome has nine *AtATG8s*, whereas yeast has just one *ATG8*. The nine *AtATG8s*<sup>10,11</sup> and the eight *AtATG18s*<sup>7</sup> show differential expression patterns, indicating their diverse roles. Although extensive studies have revealed the roles of some ATGs and the underlying mechanisms in plants, there is a lack of systematic analysis of ATGs in plants and their expression patterns under normal growth and stress conditions. In this study, 33 putative rice ATGs (OsATG homologues) were identified in the rice genome, and their expression profiles under normal growth conditions and stress treatments were analysed with semi-quantitative RT-PCR and mining the rice expression database. This study gives a systematic clue to investigate the physiological functions of OsATG homologues and forms a basis for further studies of the OsATG family in rice.

## 2. Materials and methods

### 2.1. Identification of OsATG homologues

A preliminary search for OsATG homologues was performed using the key word 'autophagy' in the Rice Annotation Project Database (RAP-DB, <http://rapdb.dna.affrc.go.jp/>). Another approach was to search for OsATG homologues using BLASTP in RAP-DB and the NCBI database (<http://www.ncbi.nlm.nih.gov/>) with yeast ATG proteins downloaded from Pfam 24.0 (release October 2009) (<http://pfam.sanger.ac.uk/>). In addition, eight OsATG homologues from a previous publication<sup>9</sup> were also included in our analysis. After removing the redundant genes, all putative OsATG homologues were searched in the Pfam database to confirm the presence of ATG domains. The corresponding full-length cDNAs and the predicted proteins of these OsATG homologues were downloaded from the KOME full-length cDNA database (<http://cdna01.dna.affrc.go.jp/cDNA/>) or NCBI. The information of all the analysed putative OsATG homologues is listed in Supplementary Table S1.

### 2.2. Chromosomal localization and gene duplication

The OsATG homologues were positioned on the rice chromosomes using BLASTN at the Rice Genome Annotation Project website (MSU-RGA, [http://rice.plantbiology.msu.edu/analyses\\_search\\_blast.shtml](http://rice.plantbiology.msu.edu/analyses_search_blast.shtml)). The OsATG homologues present on the duplicated chromosomal segments were identified by segmental genome duplication of rice available at MSU-RGA with the maximum distance permitted between collinear gene pairs of 100 kb. The OsATG homologues separated by a maximum of five genes were identified as tandem duplicated genes.

### 2.3. Protein sequence alignment and phylogenetic analysis

Multiple sequence alignments of amino acid sequences were performed using ClustalX (version 2.0.9). The unrooted phylogenetic trees were generated by the neighbour-joining (NJ) method using ClustalX and with the *p*-distance substitution model in MEGA 4.<sup>12</sup> Bootstrap analysis was performed with 1000 replicates to obtain a support value for each branch.

### 2.4. Analysis of gene and protein structure

Scans for the active sites of OsATG homologues were performed using PROSITE (<http://www.expasy.ch/tools/scanprosite/>). Exon-intron organization was determined using the genome browser tool in RAP-DB. Gene structure was manually assessed for each predicted OsATG homologue. The isoelectric point and molecular weight were estimated using the

tools from ExpASY (<http://us.expasy.org/tools/protparam.html>).

### 2.5. Plant materials and growth conditions

The rice cultivar Zhonghua 11 (*Oryza sativa* L. *japonica*) was used in this study. For expression analyses of *OsATG* homologues under normal conditions, total RNA was extracted from different tissues of the rice plants, grown in the natural field of South China Botanical Garden.

For various treatments, seeds were soaked in water and germinated at 28°C for 2 days and then grown in Hoagland's solution<sup>13</sup> for 3 weeks. For salt treatment, 3-week-old seedlings were grown in Hoagland's solution containing 250 mM NaCl for 4 h; for cold treatment, the seedlings were kept at 4°C for 4 h; for drought treatment, the seedlings were dried for 4 h between folds of tissue paper at 28 ± 1°C; for carbohydrate starvation, the seedlings were kept in the dark for 48 h; for gibberellic acid (GA<sub>3</sub>), 2,4-dichlorophenoxyacetic acid (an auxin; 2,4-D), kinetin (a cytokinin; KT), or abscisic acid (ABA) treatment, the seedlings were cultured in Hoagland's solution containing 5 μM GA<sub>3</sub>, 5 μM 2,4-D, 5 μM KT, or 25 μM ABA, respectively, for 24 h.

For nitrogen treatment, Zhonghua 11 seeds were sterilized with 70% ethanol for 1 min, followed by 2.5% sodium hypochlorite containing one drop of Tween 20 per 50 ml for 25 min, then rinsed five times with sterile distilled water. The sterilized seeds were inoculated on 1/2 MS solid medium<sup>14</sup> containing 1% sucrose and cultured under a 16/8 h light/dark cycle for 10 days. On the 10th day, some rice seedlings were washed and subcultured on NO<sub>3</sub><sup>-</sup>-free solid medium for 7 days. NO<sub>3</sub><sup>-</sup>-free medium was a modification of MS salts in which the macronutrient composition was changed to 3 mM KCl, 0.15 mM CaCl<sub>2</sub>, 0.075 mM MgSO<sub>4</sub>, 0.0625 mM KH<sub>2</sub>PO<sub>4</sub>, 0.5 mM NH<sub>4</sub>Cl, and 0.5 mM succinic acid. Within 7 days, two changes of medium were made to deplete stored nitrate in the plants. After that, some seedlings were subcultured into liquid nitrate induction medium. NaNO<sub>3</sub> was added to a final concentration of 25 mM for nitrate induction, and plants were collected at a series of time points. For ammonium induction, NO<sub>3</sub><sup>-</sup>-free medium used on the 10th day was replaced by nitrogen starvation solution (NO<sub>3</sub><sup>-</sup>-free medium minus 0.5 mM NH<sub>4</sub>Cl), and 5 mM NH<sub>4</sub>Cl was used as the nitrogen source. After collection, all samples were flash-frozen in liquid nitrogen and stored at -80°C for subsequent RNA extractions. The seedlings were grown in normal MS medium as a control.

The growth conditions, treatments, and experiments on the plant materials in the digital expression database could be referenced to published

papers<sup>15,16</sup> and the web page (<http://bioinformatics.med.yale.edu/riceatlas/overview.jsp>).

### 2.6. Semi-quantitative RT-PCR analysis

Total RNA was extracted using Trizol reagent according to the manufacturer's instructions (Invitrogen, <http://www.invitrogen.com>). First-strand cDNA was synthesized from 3 μg of total RNA from each sample using M-MLV reverse transcriptase (Promega, <http://www.promega.com>). The first-strand cDNA was used as a template for semi-quantitative PCR analysis after normalization using rice *Actin1* (accession no. AB047313). The appropriate amount of template cDNA and number of PCR cycles were determined for each gene to ensure that amplification occurred in the linear range and that amplified products were quantified accurately. All primer sequences used in this study are listed in Supplementary Table S2. To ensure that the primers were specific for the correct *OsATG* homologues, primers were designed using software Primer Premier v5.00 (PREMIER Biosoft International). Some of the amplification products obtained with the different primer pairs were purified from the gel and sequenced, then the sequences were aligned on the RAP-DB website to make sure that they were specific. The PCR products were analysed on 1% agarose gels stained with ethidium bromide and visualized using the Fluorescence Chemiluminescence and Visible Imaging System. The RT-PCR bands were digitalized using Gel-Pro Analyzer (Media Cybernetics Inc.), and the expression values of *OsATG* homologues were normalized using the band values of the rice *Actin1* gene.

### 2.7. Digital expression analysis of *OsATG* homologues

Four approaches were used in digital expression analysis of *OsATG* homologues. The Rice Expression Profile Database (RiceXPro) (<http://ricexpro.dna.affrc.go.jp/index.html>) is a repository of gene expression data derived from microarray experiments encompassing the entire life cycle of the rice plant from the germination, seedling, tillering, stem elongation, panicle initiation, booting, heading, flowering, and ripening stages.<sup>17</sup> The expression of *OsATG* homologues from this database is summarized in Supplementary Fig. S1.

Second, the massively parallel signature sequencing (MPSS) database was searched at the rice MPSS project (<http://mpss.udel.edu/rice/>) for 20-base signatures from 22 mRNA libraries representing 18 different tissues/organs in rice expression evidence analysis.<sup>15</sup> Only the signatures that uniquely identified an individual gene and showed a perfect match (100% identity over 100% of the length of the tag) were used for the analysis. The normalized abundance (tags per

million, tpm) of these signatures for a given gene in a given library represents the quantitative estimate of the expression of that gene. The tissue expression results from this database are listed in Supplementary Table S3, and the results from the rice plants infected by *Xanthomonas oryzae* and *Magnaporthe grisea* are listed in Supplementary Table S4. The results from the rice plants under abiotic stresses are listed in Supplementary Table S5.

Third, the cellular expression profile data of OsATG homologues were extracted from Yale Virtual Center for Cellular Expression Profiling<sup>16</sup> of Rice (<http://bioinformatics.med.yale.edu/riceatlas/overview.jsp>) using gene locus IDs. This analysed result is listed in Supplementary Tables S6–S9.

Fourth, the rice microarray data were extracted from Gene Expression Omnibus (GEO) database (<http://www.ncbi.nlm.nih.gov/geo/>) using OsATG locus IDs. The data from the series accession number GSE4471 were the expression profiles of 1-week-old roots from rice varieties Azucena and Bala following treatment with 1 ppm sodium arsenate.<sup>18</sup> The data from GSE3053 were the expression data from salt-tolerant (FL478) and salt-sensitive (IR29) rice plants treated with salt.<sup>19</sup> The data from GSE5167 were the expression profile when the rice was treated with cytokinin.<sup>20</sup> The OsATG expression results from these data are listed in Supplementary Table S10.

## 2.8. *Ka/Ks analysis and calculation of the dates of the duplication events*

The number of non-synonymous substitutions per non-synonymous site (*Ka*) and the number of

synonymous substitutions per synonymous site (*Ks*) of duplicated genes were analysed by DnaSP Version 5. The dates of the duplication events were calculated by the equation  $T = Ks/2\lambda$ , for rice,  $\lambda = 6.5 \times 10^{-9}$ .<sup>21,22</sup>

## 3. Results and discussion

### 3.1. Identification of 33 OsATG homologues in the rice genome

Numerous studies in *A. thaliana* have suggested that autophagic processes occur in plants;<sup>2</sup> however, the knowledge of ATGs in plants is still lacking. The availability of complete rice genome sequences provides the possibility of identifying OsATG family members in rice. Here, we identified a total of 33 putative OsATG homologues in rice (Supplementary Table S1, Fig. 1). All of them were predicted to play roles in the autophagy process, including from the first step of induction to the last step of vesicle fusion with the vacuole/lysosome.<sup>1</sup> Among the 33 OsATG homologues, 23 were identified from RAP-DB build 5: OsATG1a, OsATG1b, OsATG1c, OsATG3b, OsATG4b, OsATG5, OsATG6a, OsATG6b, OsATG7, OsATG8d, OsATG8e, OsATG8f, OsATG9a, OsATG9b, OsATG13a, OsATG13b, OsATG16, OsATG18a, OsATG18b, OsATG18c, OsATG18d, OsATG18e, and OsATG18f. Eight (OsATG3a, OsATG4a, OsATG8a, OsATG8b, OsATG8c, OsATG10a, OsATG10b, and OsATG12) were cited from Chung *et al.*<sup>9</sup> Then we used the above OsATG proteins as queries to search NCBI (<http://www.ncbi.nlm.nih.gov/>) by BLASTP and finally identified two other OsATG homologues, OsATG6c and OsATG8i. However, OsATG8i could not

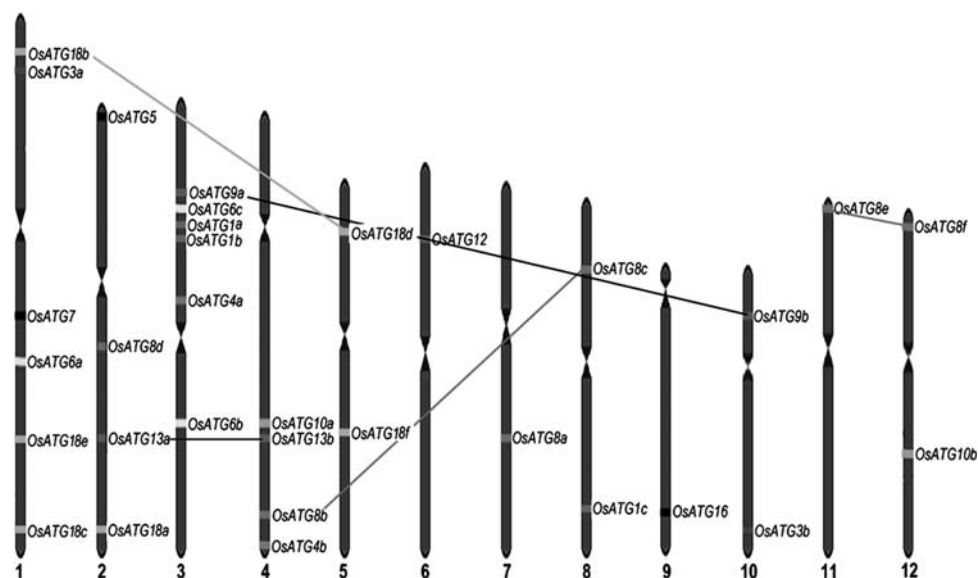


**Figure 1.** Localization of the rice autophagy-associated homologues on rice chromosomes. OsATG homologues classified into different subfamilies are shown in different colours. (For interpretation of the references to color in this figure legend, the reader is referred to the web version of the article.) Chromosome number is indicated at the bottom of each chromosome. The OsATG homologues present on duplicated chromosomal segments between two chromosomes are connected by lines.



with high bootstrap values (Fig. 2B–D, F–H). In addition, the members of these six subfamilies had similar gene structures within their subfamilies (Supplementary Fig. S3). These data suggest that the member diversification within the six *ATG* subfamilies might have occurred after the divergence of monocots and dicots. Further, the two members of each of the *OsATG3*, *OsATG4*, and *OsATG10* subfamilies were not split by other monocots (Fig. 2B, C, and G), indicating that their member divergence occurred after the divergence of the cereals. On the other hand, the two members of each of the *OsATG9* and *OsATG13* subfamilies were split by other monocots, suggesting that the member diversification of the *OsATG9* and *OsATG13* subfamilies might have occurred before the divergence of the cereals (Fig. 2F and H). Within the *ATG6* subfamily (Fig. 2D), the phylogenetic relationship of *OsATG6b* to *OsATG6c* was closer than either of them to *OsATG6a*, suggesting that the diversification of *OsATG6a* from *OsATG6b* and *OsATG6c* might have occurred earlier than the divergence of *OsATG6b* from *OsATG6c*.

We found that the *OsATG* homologues of the other three *ATG* subfamilies (*ATG1*, *ATG8*, and *ATG18*) were split by dicots. Within the *ATG1* subfamily (Fig. 2A), *OsATG1a* was separated from *OsATG1b* and *OsATG1c* by the dicots, but *OsATG1b* and *OsATG1c* were clustered tightly. This indicates that the divergence of *OsATG1a* from *OsATG1b* and *OsATG1c* might have occurred before the diversification of the monocots and the dicots, but *OsATG1b* and *OsATG1c* might have diverged after the diversification of the monocots and dicots (Fig. 2A). Within the *OsATG8* subfamily (Fig. 2E), seven *OsATG8s* were clustered into three groups (I: *OsATG8a*; II: *OsATG8b* and *OsATG8c*; III: *OsATG8d*, *OsATG8i*, *OsATG8f*, and *OsATG8e*), and the three groups were split by the dicots, indicating that the divergence of the three groups might have occurred before the divergence of the monocots and dicots. *OsATG8b* and *OsATG8c* of Group II were split by the monocots but not by the dicots, which indicates that the divergence of *OsATG8b* and *OsATG8c* might have occurred after the divergence of the monocots and dicots and before the divergence of

the cereals. The four members of Group III (*OsATG8d*, *OsATG8i*, *OsATG8f*, and *OsATG8e*) were split by the dicots, which suggests that the divergence of *OsATG8d* and *OsATG8i* from *OsATG8f* and *OsATG8e* might have occurred before the divergence of the monocots and dicots. The phylogenetic distances from Group III to Groups I and II were large, indicating that the divergence of *OsATG8d*, *OsATG8i*, *OsATG8f*, and *OsATG8e* from *OsATG8a*, *OsATG8b*, and *OsATG8c* might have occurred very early. Within the *ATG18* subfamily (Fig. 2I), six *OsATG* homologues could also be clustered into three groups, which were split by the dicots, indicating that the divergence of the three groups of the *ATG18* subfamily might have occurred before the divergence of the monocots and dicots. With Group II of the *ATG18* subfamily, *OsATG18b*, *OsATG18c*, and *OsATG18d* were mixed with the *ATGs* of dicots and monocots, suggesting that their divergence might have occurred before the divergence of the monocots and dicots; however, two members of Group III (*OsATG18e* and *OsATG18f*) were clustered into the monocots, suggesting that their divergence might have occurred after the divergence of the monocots and dicots.

### 3.3. *Ka/Ks* analysis and calculation for the date of the duplication events

The *Ka/Ks* ratio is a measure to explore the mechanism of gene divergence after duplication.  $Ka/Ks = 1$  means neutral selection,  $Ka/Ks < 1$  means purifying selection, and  $Ka/Ks > 1$  means accelerated evolution with positive selection.<sup>24</sup> We calculated six duplicated pairs in the *ATG* family (Table 1). The *Ka/Ks* ratios of *OsATG13a/OsATG13b*, *OsATG8b/OsATG8c*, *OsATG8e/OsATG8f*, and *OsATG1a/OsATG1b* were  $< 1$ , suggesting purifying selection on these four duplicated pairs. For the other two duplicated pairs, *OsATG9a/OsATG9b* and *OsATG18a/OsATG18d*, the *Ka/Ks* ratios were  $> 1$ , suggesting positive selection on the two duplicated pairs.

We also calculated the dates of the duplication events (Table 1). All duplication events occurred after the origin of the grasses.<sup>25,26</sup> Duplication events for the pairs *OsATG8b/OsATG8c* and *OsATG8e/OsATG8f*

**Table 1.** *Ka/Ks* analysis and estimate of the absolute dates for the duplication events between the duplicated *OsATG* homologues

Duplicated pair	Ks	Ka	Ka/Ks	Duplicate type	Purifying selection	Date (million years)
<i>OsATG9a/OsATG9b</i>	0.2447	0.3512	1.4352	Segmental	No	18.82
<i>OsATG13a/OsATG13b</i>	0.6755	0.2585	0.3826	Segmental	Yes	51.96
<i>OsATG18a/OsATG18d</i>	0.2786	0.4118	1.4781	Segmental	No	21.43
<i>OsATG8b/OsATG8c</i>	0.8681	0.0259	0.0298	Segmental	Yes	66.77
<i>OsATG8e/OsATG8f</i>	0.7662	0.5358	0.6992	Segmental	Yes	58.93
<i>OsATG1a/OsATG1b</i>	0.6167	0.5278	0.8558	Tandem	Yes	47.43

occurred within last 70–55 million years, according to the first whole-genome duplication events of grass genomes.<sup>27,28</sup> Latest duplication event was the duplication of *OsATG18a/OsATG18d* among all the duplicated *OsATG* homologues, which might occur ~21.43 million years ago.

### 3.4. Differential expression of *OsATG* homologues under normal growth conditions

Autophagy plays critical roles during cellular development and differentiation and may be linked to life-span extension,<sup>1</sup> even under normal growth conditions without the imposition of environmental stresses.<sup>4,6</sup> Three approaches were used to investigate the expression of *OsATG* homologues in various organs or in different cell types and at different developmental stages. First, semi-quantitative RT–PCR amplified all 33 *OsATG* homologues from at least one tissue when the rice plants were grown under normal conditions from the seedling stage to the booting stage (Fig. 3), including the three *OsATG* homologues (*OsATG6c*, *OsATG8d*, and *OsATG8f*) whose corresponding mRNAs could not be found in GenBank (Supplementary Table S1). At the booting stage, 22 genes were expressed in all five tested organs: roots, culms, flag leaf blades, young panicles, and leaf sheaths. The other 11 genes were expressed in one to four tissues. At the seedling stage, all 33 *OsATG* homologues were expressed in roots, culms, and leaf blades. Notably, the expression patterns of some *OsATG* homologues showed differences from the seedling stage to the booting stage, such as *OsATG3a* being expressed in the culms of the seedlings but not in the culms of the booting plants. Second, the expression data of 22 *OsATG* homologues could be extracted using the gene locus ID search from the leaf expression profiles throughout the entire growth period in the field at RiceXPro,<sup>17</sup> and their expression data were used to construct a heatmap. The heatmap showed that all 22 *OsATG* homologues were expressed in at least one growth stage throughout life (Supplementary Fig. S1). Notably, their expression levels were not very high in the chip data. Third, the Yale Virtual Center for Cellular Expression Profiling of Rice<sup>16</sup> was also used to analyse the cellular expression of the *OsATG* homologues available in this database. In most tissues, the *OsATG* homologues were expressed in nearly all cell types, from the scutellum to the radicle of the germinating rice seeds (Supplementary Table S6), the different meristem tissues (Supplementary Table S7), from the bulliform to the vein of the leaves (Supplementary Table S8), and from the lateral root cap to the vascular bundle of the roots (Supplementary Table S9). All of these data indicate that the *OsATG* homologues are

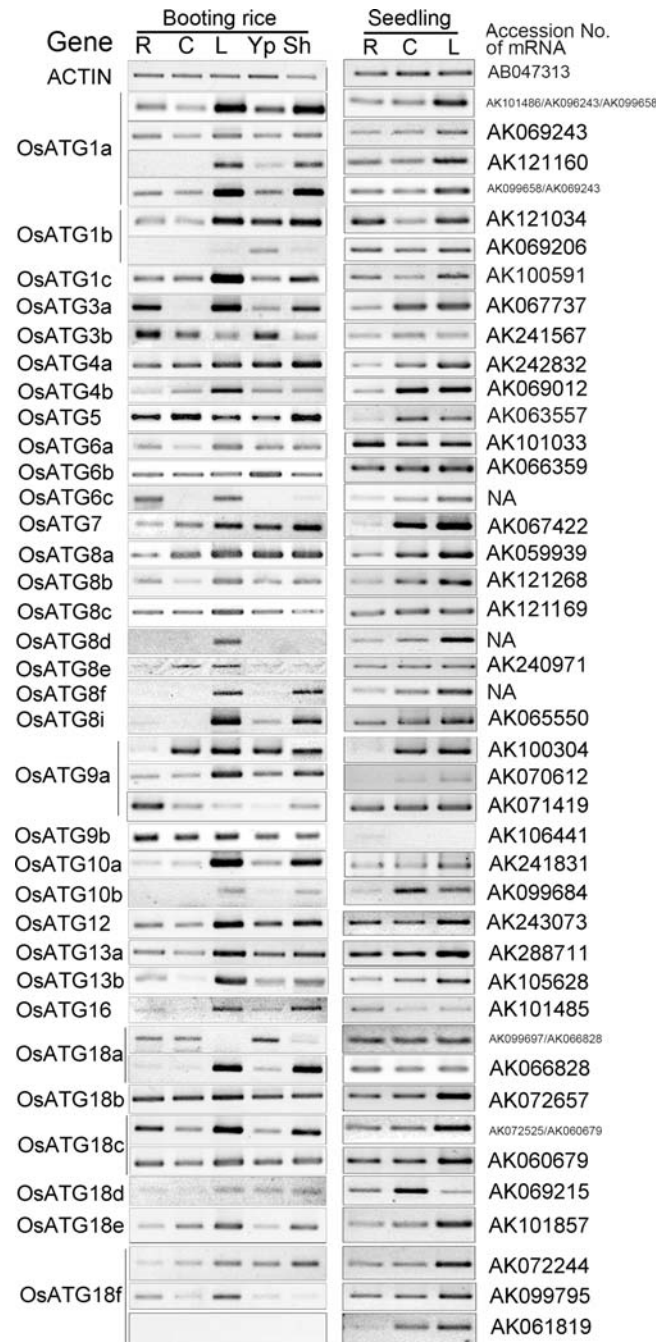


**Figure 3.** Expression profiles of *OsATG* homologues in various rice organs at the booting stage and the seedling stage by semi-quantitative RT–PCR. Total RNAs were from different organs when the rice plants were grown under normal growth conditions. R, roots; C, culms; L, leaf blades; Yp, young panicles; Sh, leaf sheaths. The accession numbers of mRNAs on the right side indicate that the bands from RT–PCR were actually amplified by the primers, and the NA indicates that this gene has no mRNA record in GenBank.

expressed in different typical cells of all rice tissues at various developmental stages.

Transgenic *Arabidopsis* plants with five *AtATG8* promoters have shown that in plants, the cellular processes involving the *AtATG8* genes function

efficiently in young, non-senescing tissues, both under favourable growth conditions and under starvation stress.<sup>29</sup> The expression analyses of *OsATG* homologues under normal conditions provided a strong indication of the roles of autophagy in plant cell development and differentiation even under normal growth conditions. However, the roles of plant autophagy under normal conditions have come into question because of the lack of an obvious growth phenotype of the *ATG* mutants.<sup>30</sup> This sharply contrasts with their animal counterparts.<sup>4</sup> The reasons for this distinction may be as follows. Most plants have several homologues of each *ATG* gene. For example, rice has seven *OsATG8* homologues and eight *OsATG18* homologues,<sup>7</sup> respectively, and their homologues, such as *OsATG8a*, *OsATG8b*, and *OsATG8c*, are sometimes expressed at the same time in the same tissues (Fig. 3, Supplementary Table S3). This may result in functional complementation for a single *ATG* mutant. However, disruption of the *Arabidopsis* single-copy gene *ATG5* or *ATG7* also produces no phenotype under normal conditions;<sup>31</sup> therefore, other, unknown mechanisms may explain the lack of *ATG* mutant phenotypes in plants.

However, by analysing the cycle numbers in semi-quantitative RT-PCR and the digital expression data (Supplementary Table S3), we found differences in the expression levels of some *OsATG* homologues. *OsATG8a*, *OsATG8b*, and *OsATG8c* were expressed more highly than *OsATG8e* (Fig. 3, Supplementary Table S3). Further, we found that an *OsATG8b* mutant showed the phenotype of delayed flowering time in rice, but it lacked an obvious growth phenotype under normal growth conditions (data not shown). *OsATG10a* and *OsATG10b* share significant sequence similarity and are ubiquitously expressed in all organs,<sup>32</sup> but we found that they were expressed differently in the organs at the booting developmental stage (Fig. 3). Nine *AtATG8s* of *Arabidopsis* also show distinct spatial and temporal expression patterns in roots and in young, non-senescing tissues, both under favourable growth conditions and under starvation stresses.<sup>29</sup> These observations indicate that the different *ATG* homologues, even within the same *ATG* subfamily, might play various roles in rice even under normal growth conditions.

### 3.5. Differential expression of *OsATG* homologues in response to hormone treatments

To monitor the responses of *OsATG* homologues to various hormones, their expression was investigated by semi-quantitative RT-PCR. A total of 31 *OsATG* homologues could be amplified in 3-week-old rice seedlings subjected to various hormone treatments, including 2,4-D, KT, ABA, and GA<sub>3</sub>. The fold-change

values of the *OsATG* homologues are given in Fig. 4, considering the expression levels of the control (water) as 1. Thirty *OsATG* homologues showed differential expression in at least one pair of tissues or at least one hormone treatment compared with the control, except *OsATG8c*. However, the expression response patterns of these *OsATG* homologues to hormones were complex. Most of the *OsATG* homologues showed various degrees of down-regulation by GA<sub>3</sub>, but the alternatively spliced AK070612 mRNA form of *OsATG9a* was up-regulated by at least 8-fold in all the three organs (Fig. 4H). For the other three hormone treatments, the *OsATG* homologues exhibited differential patterns of up- and down-regulation. Interestingly, some *OsATG* homologues showed different responses to the same hormone in various organs. For example, the expression of *OsATG8d* was down-regulated about 10-fold in roots, while it was up-regulated at least 5-fold in sheathes and more than 2-fold in leaves after 2,4-D treatment (Fig. 4G). The digital expression results after KT treatment were analysed, and they were consistent with our semi-quantitative RT-PCR results (Supplementary Table S10).

Little published information is available regarding the relationships among the *OsATG* homologues and hormonal responses. Our results clearly show that *OsATG* homologues might play important roles in responses to various plant hormones. Jain *et al.*<sup>33</sup> postulated that disruption of cytokinin flux to detached leaves triggers the selective degradation of carbonylated proteins via autophagy. Our results may have implications for the linkage between autophagy and hormones in the control of protein mobilization and in response to changes in nitrogen availability.

### 3.6. Differential expression of *OsATG* homologues in response to stress treatments

To gain insight into the comprehensive roles of *OsATG* family members in response to various stresses, their expression patterns were investigated in rice seedlings subjected to salt, drought, cold, and dark treatments by semi-quantitative RT-PCR (Fig. 5). The responses of *OsATG* homologues to arsenate and salt stresses (Supplementary Tables S5 and S10) were also analysed using the digital expression data. Among 31 *OsATG* homologues, 30 showed differential expression in at least one tissue or at least one stress treatment compared with the control, and only the alternatively spliced AK069243 form of *OsATG1a* and *OsATG16* did not show differential expression in response to any stress treatments (Fig. 5A and L), when judged by at least 2-fold increased or decreased expression change. Some *OsATG* homologues were only regulated by a specific stress condition;



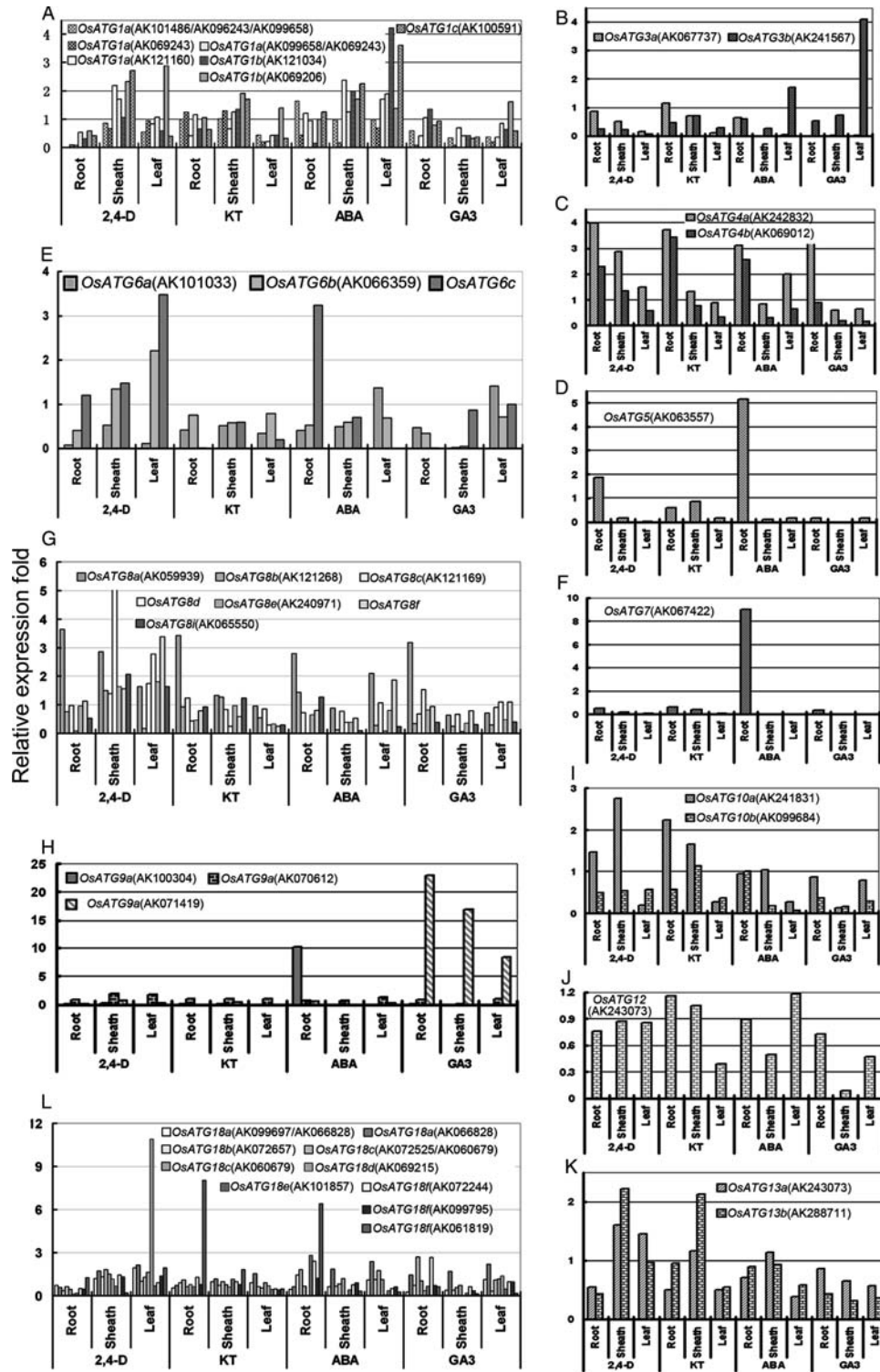


**Figure 4.** Semi-quantitative RT–PCR analysis of the relative expression levels of rice *OsATG* homologues under various hormone treatments. Three-week-old seedlings were irrigated with Hoagland’s solution containing 5  $\mu$ M gibberellic acid (GA<sub>3</sub>), 5  $\mu$ M 2,4-dichlorophenoxyacetic acid (2,4-D), 5  $\mu$ M KT, or 25  $\mu$ M ABA for 24 h. Expression levels in treated seedlings were normalized to those of the water-treated seedlings, whose expression levels were defined as 1. A gene name with two or more mRNA accession numbers in the parentheses indicates that this set of primers could amplify two or more alternatively spliced mRNA forms; a gene name without an mRNA accession number indicates that this gene has no mRNA record in GenBank; the same applies to Figs 5 and 6.

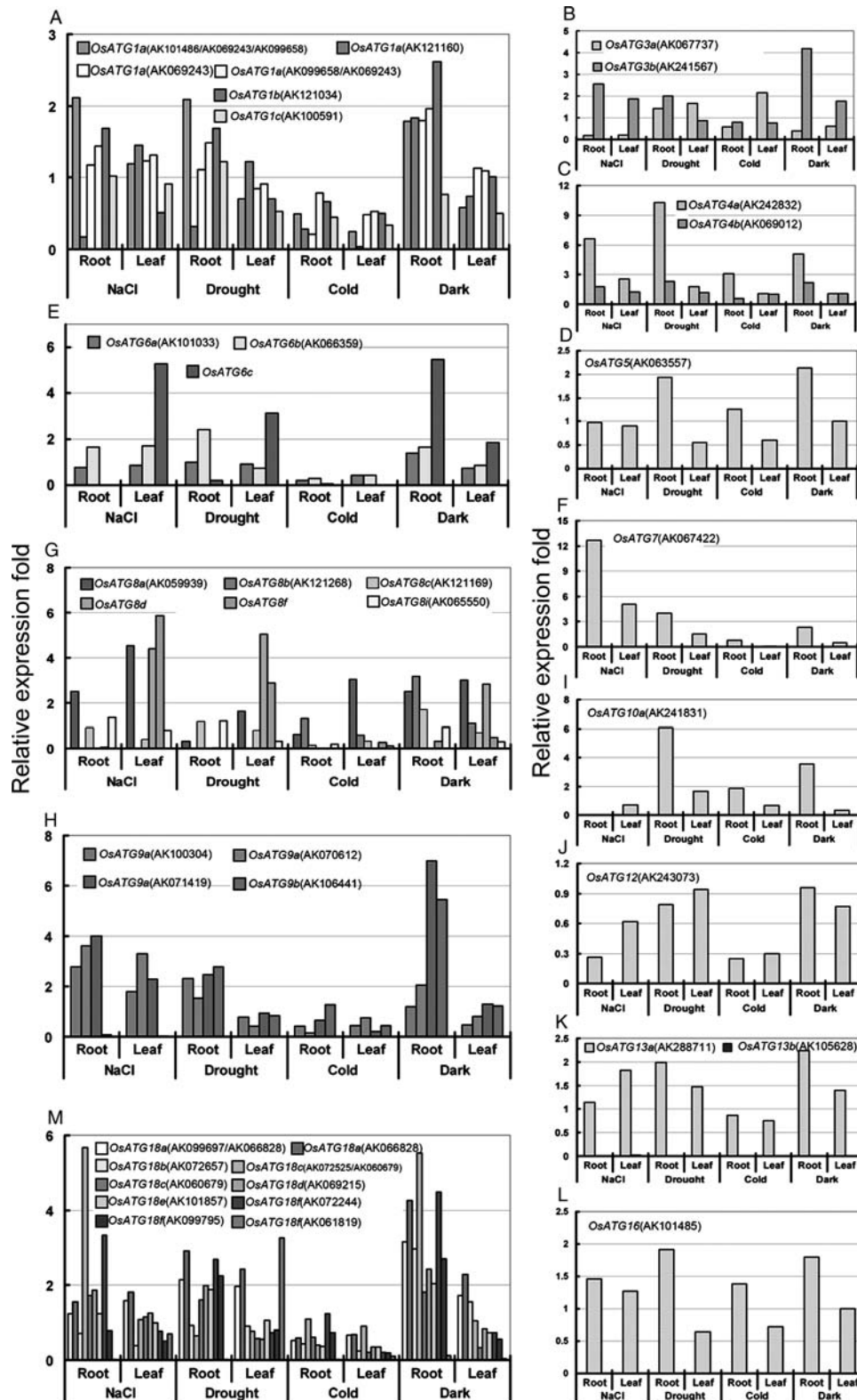


**Figure 5.** Relative expression levels of rice *OsATG* homologues under abiotic stresses. Three-week-old rice seedlings under normal growth conditions were the control. Expression levels in treated seedlings were normalized to those of the control seedlings, whose expression levels were defined as 1. For salt treatment, the seedlings were kept in a 250 mM NaCl solution for 4 h. For drought treatment, seedlings were dried for 4 h between folds of tissue paper at  $28 \pm 1^\circ\text{C}$ . For cold treatment, the seedlings were kept at  $4 \pm 1^\circ\text{C}$  for 4 h. For dark treatment, seedlings were kept in the dark for 48 h.

however, others were regulated by more than one stress condition.

In response to salt treatment, 13 *OsATG* homologues (*OsATG1a*, *OsATG4a*, *OsATG6c*, *OsATG7*, *OsATG8a*, *OsATG8d*, *OsATG8f*, *OsATG9a*, *OsATG18a*, *OsATG18c*, *OsATG18d*, *OsATG18e*, and *OsATG18f*) were up-regulated and 13 *OsATG* homologues (*OsATG1a*, *OsATG3a*, *OsATG6c*, *OsATG8b*, *OsATG8c*, *OsATG8f*, *OsATG9b*, *OsATG10a*, *OsATG12*, *OsATG13b*, *OsATG18b*, and *OsATG18f*) were down-regulated (Fig. 5). Notably, the expression changes of the different alternatively spliced mRNA forms of *OsATG3a* showed different response to the salt treatment, and the expression changes of *OsATG6c*, *OsATG8d*, and *OsATG* in the roots and the leaves showed different response to the salt treatment. In response to drought treatment, 13 *OsATG* homologues (*OsATG1a*, *OsATG3b*, *OsATG4a*, *OsATG4b*, *OsATG6b*, *OsATG6c*, *OsATG7*, *OsATG8d*, *OsATG8f*, *OsATG9a*, *OsATG9b*, *OsATG18a*, and *OsATG18f*) were up-regulated and 9 *OsATG* homologues (*OsATG1a*, *OsATG6c*, *OsATG8a*, *OsATG8b*, *OsATG8d*, *OsATG8f*, *OsATG8i*, *OsATG13b*, and *OsATG18f*) were down-regulated. In response to cold treatment, most (21) of the *OsATG* homologues were down-regulated and three genes (*OsATG3a*, *OsATG4a*, and *OsATG8a*) were up-regulated, only 10 *OsATG* homologues (*OsATG1b*, *OsATG3b*, *OsATG4b*, *OsATG5*, *OsATG8b*, *OsATG10a*, *OsATG13a*, *OsATG16*, *OsATG18a*, and *OsATG18c*) did not respond to the cold treatment. In response to 48 h dark treatment, 19 *OsATG* homologues were up-regulated and 8 *OsATG* homologues were down-regulated. Notably, the expression changes of *OsATG8d* in the roots and the leaves showed different response to the dark treatment, and six *OsATG* homologues (*OsATG1a*, *OsATG6a*, *OsATG6b*, *OsATG8c*, *OsATG12*, and *OsATG16*) did not respond to the dark treatment. Through mining the digital expression data, only *OsATG5* and *OsATG18e* showed differential expression under arsenate treatment (Supplementary Table S10).

We also analysed the responses of *OsATG* homologues to infection with *M. grisea* or *X. oryzae*, which causes severe loss to rice yield. We mined the rice expression database to determine their expression fold changes (Supplementary Table S4). The microarray data and the infection with *M. grisea* or *X. oryzae* were published previously.<sup>15</sup> We found that some *OsATG* homologues (*OsATG3a*, *OsATG3b*, *OsATG4b*, and *OsATG18e*) showed differential responses to the disease infection between the resistant and the susceptible reactions.

High salt and osmotic stresses induce autophagy in an *A. thaliana*, and autophagy-defective RNAi-*AtATG18a* plants are more sensitive to salt and drought conditions than wild-type plants, demonstrating a role for autophagy in response to these

stresses.<sup>34</sup> Recent evidence suggests that autophagy is also necessary for the proper regulation of hypersensitive response-programmed cell death during the plant innate immune response.<sup>35–37</sup> Together, these data suggest that autophagy plays roles in the responses of plants to biological and abiotic stresses.

### 3.7. Differential expression of *OsATG* homologues under nitrogen and carbon starvation

In plants, autophagy is important for nutrient remobilization during sugar and nitrogen starvation and leaf senescence.<sup>37,38</sup> To gain insight into the roles of *OsATG* homologues during nitrogen starvation conditions, their expression patterns were investigated in rice seedlings subjected to  $\text{NH}_4^+$  and  $\text{NO}_3^-$  starvation (Fig. 6I and II). For 48 h nitrate starvation, 18 *OsATG* homologues were up-regulated and 10 *OsATG* homologues were down-regulated in at least one organ. For 48 h ammonium starvation, 18 *OsATG* homologues were up-regulated and 8 *OsATG* homologues were down-regulated in at least one organ (Fig. 6I and II). Notably, the expression change of some *OsATGs* was different in response to ammonium and nitrate treatments. The most-changed expression levels in response to ammonium included AK069206 of *OsATG1a*, AK069012 of *OsATG4b*, *OsATG8d* and AK072244 of *OsATG18f* (Fig. 6IA, C, G, and M); however, the most-changed expression levels in response to nitrate treatment were AK069243 of *OsATG1a*, *OsATG6c*, *OsATG8d*, and AK072244 of *OsATG18f* (Fig. 6IIA, B, G, and M).

Autophagy is triggered by carbohydrate starvation in rice and tobacco-cultured cells.<sup>38,39</sup> Dark stress induces carbohydrate starvation and triggers a profound metabolic and structural rearrangement.<sup>40</sup> Autophagy has been characterized at both the biochemical and structural levels in carbohydrate-starved plant cells. To monitor the responses of *OsATG* homologues to dark-induced carbohydrate starvation, we analysed the expression changes of *OsATG* homologues when the rice plants were kept in the dark for 48 h. We found that 17 *OsATG* homologues were up-regulated and 10 *OsATG* homologues were down-regulated by dark treatment (Fig. 5). Notably, 15 *OsATG* homologues were up-regulated only in the roots, but not in the leaves, while *OsATG8a* and *OsATG18a* were up-regulated in both the roots and the leaves after 48 h dark treatment (Fig. 5). In *Arabidopsis*, *AtATG4a*, *AtATG4b*,<sup>41</sup> and *AtATG9*<sup>5</sup> are up-regulated in response to dark-induced carbohydrate starvation. In rice, *OsATG4a*, *OsATG4b*, *OsATG9a*, and *OsATG9b* were up-expressed by dark treatment, indicating that they are involved in dark-induced carbohydrate starvation. Our results indicate that as in other plants, most *OsATG*

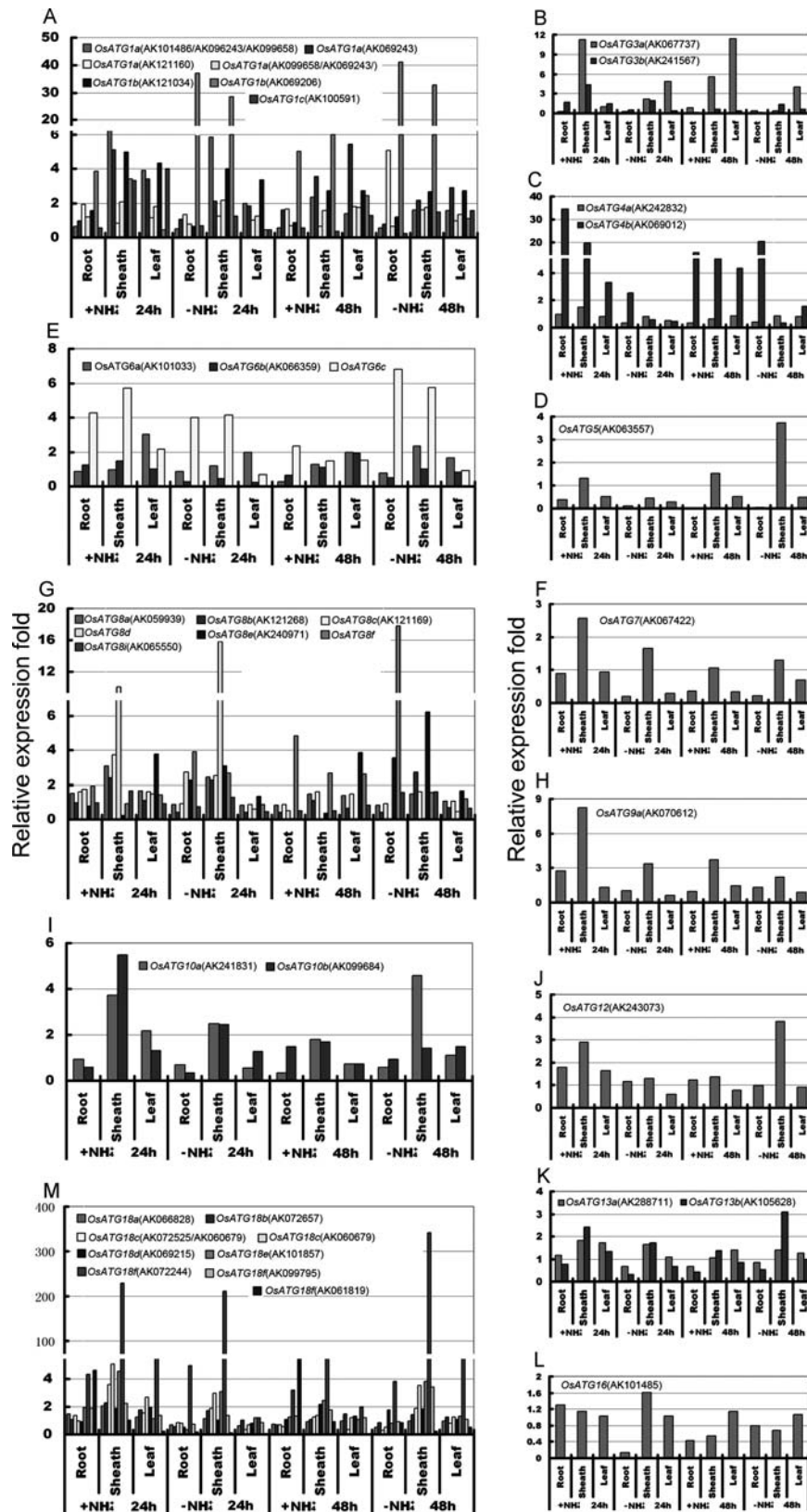


**Figure 6.** Relative expression levels of *OsATG* homologues in response to ammonium (I) and nitrate (II) treatments. Ten-day-old seedlings were transferred to nitrogen-free medium ( $-\text{NH}_4^+$  or  $-\text{NO}_3^-$ ) containing modified MS salts for 7 days for nitrogen starvation, then part of these seedlings were transferred to MS medium containing  $\text{NH}_4^+$  or  $\text{NO}_3^-$  ( $+\text{NH}_4^+$  or  $+\text{NO}_3^-$ ) as the nitrogen source. Total RNAs were extracted from these treated seedlings for RT-PCR. Expression levels in treated seedlings were normalized to those of the control seedlings grown under normal conditions, whose expression levels were defined as 1.

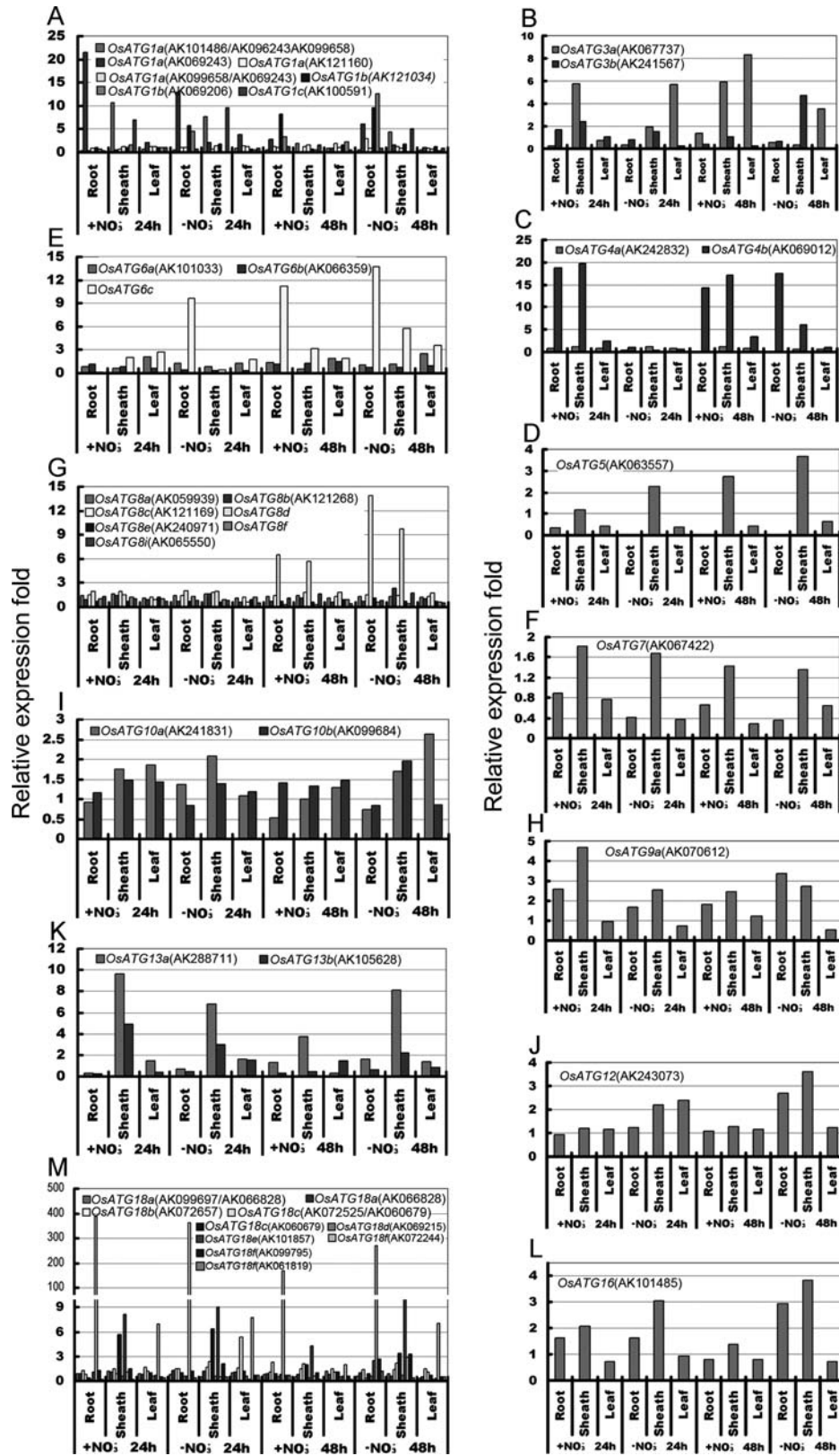


Figure 6. *Continued*

homologues are required to maintain cellular viability under nutrient-limited conditions and for efficient nutrient use in the whole plant.<sup>7</sup>

### 3.8. Expression divergence of duplicated OsATG homologues

Gene duplication leads to functional redundancy and diversification.<sup>42</sup> Under normal conditions (Fig. 3), the tandem duplicated pair *OsATG1a* and *OsATG1b* was both alternatively spliced and showed various expression patterns among the different alternative splice forms. The pair *OsATG8b* and *OsATG8c* did not show significant expression difference. For the pair *OsATG8e* and *OsATG8f*, *OsATG8e* was expressed in all tested tissues, but *OsATG8f* was only expressed in the leaf blades and the leaf sheaths at the booting stage. For the pair *OsATG9a* and *OsATG9b*, *OsATG9a* was alternatively spliced, but *OsATG9b* was not. For the pair *OsATG13a* and *OsATG13b*, *OsATG13b* was expressed more weakly than *OsATG13a* in the roots and culms. For the pair *OsATG18b* and *OsATG18d*, *OsATG18b* was expressed more strongly than *OsATG18d*. These data suggest that the duplicated OsATG homologues show differential expression patterns in normal nature fields (Fig. 3).

For the tandem duplicated pair *OsATG1a* and *OsATG1b*, their different alternatively spliced mRNA forms showed different responses to various treatments (Figs 4–6). For the segmental-duplicated pair *OsATG8b* and *OsATG8c*, *OsATG8b* was down-regulated by drought, salt, ABA, and GA<sub>3</sub> treatments, but the expression of *OsATG8c* was not obviously changed after any of the four treatments (Figs 4 and 5G). For the pair *OsATG8e* and *OsATG8f*, their responses were similar after nitrogen treatment (Fig. 6G). For the pair *OsATG9a* and *OsATG9b*, up-regulation of *OsATG9a* expression and down-regulation of *OsATG9b* expression were observed after salt treatment (Fig. 5H). For the pair *OsATG13a* and *OsATG13b*, *OsATG13b* was substantially down-regulated after various stress treatments, but *OsATG13a* was slightly up-expressed by abiotic stresses (Fig. 5K). The pair *OsATG18b* and *OsATG18d* showed similar responses to the different treatments. Comparison of the expression profiles of the OsATG homologues in the segmentally duplicated regions and in the tandemly duplicated regions showed either similar or differential expression in the case of one of the partners, reflecting conservation, neofunctionalization, or pseudogenization after the duplication event.<sup>42</sup>

### 3.9. Conclusion

In this study, we identified 33 OsATG homologues in rice, which formed 13 ATG subfamilies and may be involved in all steps of the autophagy process, as supported by phylogeny and motif organization. Gene duplication analysis revealed that expansion of some

OsATG homologues has occurred via segmental duplication events, and all of these duplication events might occur after the origin of the grasses. The expression analysis revealed differential temporal and spatial expression patterns of OsATG homologues, which suggest their roles in regulating plant growth and development throughout the life cycle of rice. Further, we found that the expression of OsATG homologues was influenced by several environmental stimuli, including hormones, abiotic stresses, and biotic stresses, indicating their role in hormonal and stress responses. However, only the functional validation and biochemical characterization of various members will provide definitive clues about the specific roles of different classes of ATG proteins. These data provided in this study will be valuable for further in-depth functional analysis of ATGs in rice.

**Supplementary data:** Supplementary data are available at [www.dnaresearch.oxfordjournals.org](http://www.dnaresearch.oxfordjournals.org).

### Funding

This research was supported by grants CNSF31071841/30900116 from the Chinese Natural Science Foundation (CNSF), grant KSCX3-EW-N-07 from the Chinese Academy of Science, and grant (8251065005000005) from the Guangdong Natural Science Foundation.

### References

1. Yang, Z.F. and Klionsky, D.J. 2009, An overview of the molecular mechanism of autophagy. In: Levine, B., Yoshimori, T. and Deretic, V. (eds), *Autophagy in Infection and Immunity*, Springer Dordrecht Heidelberg: London, New York, pp. 1–32.
2. Thompson, A.R. and Vierstra, R.D. 2005, Autophagic recycling: lessons from yeast help define the process in plants, *Curr. Opin. Plant Biol.*, **8**, 165–73.
3. Yoshimoto, K., Takano, Y. and Sakai, Y. 2010, Autophagy in plants and phytopathogens, *FEBS Lett.*, **584**, 1350–8.
4. Chung, T., Phillips, A.R. and Vierstra, R.D. 2010, ATG8 lipidation and ATG8-mediated autophagy in *Arabidopsis* require ATG12 expressed from the differentially controlled ATG12A and ATG12B loci, *Plant J.*, **62**, 483–93.
5. Hanaoka, H., Noda, T., Shirano, Y., et al. 2002, Leaf senescence and starvation-induced chlorosis are accelerated by the disruption of an *Arabidopsis* autophagy gene, *Plant Physiol.*, **129**, 1181–93.
6. Bassham, D.C. 2007, Plant autophagy—more than a starvation response, *Curr. Opin. Plant Biol.*, **10**, 587–93.
7. Xiong, Y., Contento, A.L. and Bassham, D.C. 2005, AtATG18a is required for the formation of autophagosomes during nutrient stress and senescence in *Arabidopsis thaliana*, *Plant J.*, **42**, 535–46.

8. Fujiki, Y., Yoshimoto, K. and Ohsumi, Y. 2007, An *Arabidopsis* homolog of yeast ATG6/VPS30 is essential for pollen germination, *Plant Physiol.*, **143**, 1132–9.
9. Chung, T., Suttangkakul, A. and Vierstra, R.D. 2009, The ATG autophagic conjugation system in maize: ATG transcripts and abundance of the ATG8-lipid adduct are regulated by development and nutrient availability, *Plant Physiol.*, **149**, 220–34.
10. Yoshimoto, K., Hanaoka, H., Noda, T., et al. 2003, Analysis of AtAPG8 families in plant autophagy, *Plant Cell Physiol.*, **44**, S202.
11. Yoshimoto, K., Hanaoka, H., Sato, S., et al. 2004, Processing of ATG8s, ubiquitin-like proteins, and their deconjugation by ATG4s are essential for plant autophagy, *Plant Cell*, **16**, 2967–83.
12. Tamura, K., Dudley, J., Nei, M., et al. 2007, MEGA4: molecular evolutionary genetics analysis (MEGA) software version 4.0, *Mol. Biol. Evol.*, **24**, 1596–9.
13. Baba, S. and Takahashi, Y. 1956, Water and sand culture. In: Togari, Y. and Matsuo, T. (eds), *Laboratory Manual in Crop Science*, Nogyo-Gijitsu Kyokai: Tokyo, pp. 157–85.
14. Murashige, T. and Skoog, F. 1962, A revised medium for rapid growth and bioassay with tobacco tissue culture, *Physiol. Plant*, **15**, 473–97.
15. Nobuta, K., Venu, R.C., Lu, C., et al. 2007, An expression atlas of rice mRNAs and small RNAs, *Nat. Biotechnol.*, **25**, 473–7.
16. Jiao, Y., Tausta, S.L., Gandotra, N., et al. 2009, A transcriptome atlas of rice cell types uncovers cellular, functional and developmental hierarchies, *Nat. Genet.*, **41**, 258–63.
17. Sato, Y., Antonio, B.A., Namiki, N., et al. 2010, RiceXPro: a platform for monitoring gene expression in japonica rice grown under natural field conditions, *Nucleic Acids Res.*, **39**, D1141–8.
18. Norton, G.J., Lou-Hing, D.E., Meharg, A.A., et al. 2008, Rice-arsenate interactions in hydroponics: whole genome transcriptional analysis, *J. Exp. Bot.*, **59**, 2267–76.
19. Walia, H., Wilson, C., Condamine, P., et al. 2005, Comparative transcriptional profiling of two contrasting rice genotypes under salinity stress during the vegetative growth stage, *Plant Physiol.*, **139**, 822–35.
20. Hirose, N., Makita, N., Kojima, M., et al. 2007, Overexpression of a type-A response regulator alters rice morphology and cytokinin metabolism, *Plant Cell Physiol.*, **48**, 523–39.
21. Shiu, S.H., Karlowski, W.M., Pan, R., et al. 2004, Comparative analysis of the receptor-like kinase family in *Arabidopsis* and rice, *Plant Cell*, **16**, 1220–34.
22. Yang, Z., Zhou, Y., Wang, X., et al. 2008, Genomewide comparative phylogenetic and molecular evolutionary analysis of tubby-like protein family in *Arabidopsis*, rice, and poplar, *Genomics*, **92**, 246–53.
23. Finn, R.D., Mistry, J., Tate, J., et al. 2010, The Pfam protein families database, *Nucleic Acids Res.*, **38**, D211–22.
24. Hurst, L.D. 2002, The Ka/Ks ratio: diagnosing the form of sequence evolution, *Trends Genet.*, **18**, 486.
25. Kellogg, E.A. 2001, Evolutionary history of the grasses, *Plant Physiol.*, **125**, 1198–205.
26. Gaut, B.S. 2002, Evolutionary dynamics of grass genomes, *New Phytol.*, **154**, 15–28.
27. Salse, J., Bolot, S., Throude, M., et al. 2008, Identification and characterization of shared duplications between rice and wheat provide new insight into grass genome evolution, *Plant Cell*, **20**, 11–24.
28. Eckardt, N.A. 2008, Grass genome evolution, *Plant Cell*, **20**, 3–4.
29. Slavikova, S., Shy, G., Yao, Y., et al. 2005, The autophagy-associated Atg8 gene family operates both under favourable growth conditions and under starvation stresses in *Arabidopsis* plants, *J. Exp. Bot.*, **56**, 2839–49.
30. Moriyasu, Y. and Inoue, Y. 2008, Use of protease inhibitors for detecting autophagy in plants, *Methods Enzymol.*, **451**, 557–80.
31. Thompson, A.R., Doelling, J.H., Suttangkakul, A., et al. 2005, Autophagic nutrient recycling in *Arabidopsis* directed by the ATG8 and ATG12 conjugation pathways, *Plant Physiol.*, **138**, 2097–110.
32. Shin, J.H., Yoshimoto, K., Ohsumi, Y., et al. 2009, OsATG10b, an autophagosome component, is needed for cell survival against oxidative stresses in rice, *Mol. Cells*, **27**, 67–74.
33. Jain, V., Kaiser, W. and Huber, S.C. 2008, Cytokinin inhibits the proteasome-mediated degradation of carbonylated proteins in *Arabidopsis* leaves, *Plant Cell Physiol.*, **49**, 843–52.
34. Liu, Y., Xiong, Y. and Bassham, D.C. 2009, Autophagy is required for tolerance of drought and salt stress in plants, *Autophagy*, **5**, 954–63.
35. Seay, M., Patel, S. and Dinesh-Kumar, S.P. 2006, Autophagy and plant innate immunity, *Cell. Microbiol.*, **8**, 899–906.
36. Hofius, D., Schultz-Larsen, T., Joensen, J., et al. 2009, Autophagic components contribute to hypersensitive cell death in *Arabidopsis*, *Cell*, **137**, 773–83.
37. Yoshimoto, K., Jikumaru, Y., Kamiya, Y., et al. 2009, Autophagy negatively regulates cell death by controlling npr1-dependent salicylic acid signaling during senescence and the innate immune response in *Arabidopsis*, *Plant Cell*, **21**, 2914–27.
38. Chen, M.H., Liu, L.F., Chen, Y.R., et al. 1994, Expression of Alpha-Amylases, carbohydrate-metabolism, and autophagy in cultured rice cells is coordinately regulated by sugar nutrient, *Plant J.*, **6**, 625–36.
39. Moriyasu, Y. and Ohsumi, Y. 1996, Autophagy in tobacco suspension-cultured cells in response to sucrose starvation, *Plant Physiol.*, **111**, 1233–41.
40. Vauclare, P., Bligny, R., Gout, E., et al. 2010, Metabolic and structural rearrangement during dark-induced autophagy in soybean (*Glycine max* L.) nodules: an electron microscopy and P-31 and C-13 nuclear magnetic resonance study, *Planta*, **231**, 1495–504.
41. Wada, S., Ishida, H., Izumi, M., et al. 2009, Autophagy plays a role in chloroplast degradation during senescence in individually darkened leaves, *Plant Physiol.*, **149**, 885–93.
42. Lynch, M. and Conery, J.S. 2000, The evolutionary fate and consequences of duplicate genes, *Science*, **290**, 1151–5.